Neurobiology of Disease

Synaptic Adhesion Molecule Pcdh-γC5 Mediates Synaptic Dysfunction in Alzheimer's Disease

Yanfang Li,[1] Zhicai Chen,[1] Yue Gao,[1] Gaojie Pan,[1] Honghua Zheng,[1] Yunwu Zhang,[1] Huaxi Xu,[1,2] Guojun Bu,[1,3] and Hui Zheng[1,4]

[1]Fujian Provincial Key Laboratory of Neurodegenerative Disease and Aging Research, Institute of Neuroscience, College of Medicine, Xiamen University, Xiamen 361005 Fujian, China, [2]Neurodegenerative Disease Research Program, Sanford-Burnham Medical Research Institute, La Jolla, California 92037, [3]Department of Neuroscience, Mayo Clinic, Jacksonville, Florida 32224, and [4]Huffington Center on Aging, Baylor College of Medicine, Houston, Texas 77030

Synaptic dysfunction and neuronal excitatory/inhibitory imbalance have been implicated in Alzheimer's disease (AD) pathogenesis. Although intensive studies have been focused on the excitatory synaptic system, much less is known concerning the mechanisms mediating inhibitory synaptic dysfunction in AD. We reported previously that protocadherin-γC5 (Pcdh-γC5), a member of clustered Pcdh-γ subfamily of cadherin-type synaptic adhesion proteins, functions to promote GABAergic synaptic transmission. We reveal here that Pcdh-γC5 is enriched in vesicular GABA transporter-positive synaptic puncta and its expression levels are increased in neuronal hyperexcitation conditions, upon β-amyloid (Aβ) treatment, and in amyloid precursor protein (APP)/presenilin-1 (PS1)-transgenic mice of both sexes. This is associated with elevated levels of GABAergic proteins and enhanced synaptic inhibition. Genetic knock-down experiments showed that Pcdh-γC5 modulates spontaneous synaptic currents and Aβ-induced synaptic alterations directly. Our results support a model in which Pcdh-γC5 senses neuronal hyperexcitation to augment GABAergic inhibition. This adaptive mechanism may be dysregulated under chronic excitation conditions such as AD, leading to aberrant Pcdh-γC5 expression and associated synaptic dysfunction.

Key words: Alzheimer's disease; GABA; mice; Pcdh-γC5; synaptic transmission

Significance Statement

Synaptic dysfunction is causal for Alzheimer's disease (AD). Here, we reveal a novel pathway that contributes GABAergic synaptic dysfunction in AD mediated by protocadherin-γC5. Our study not only identifies a new mechanism mediating excitatory/inhibitory balance in AD, but may also offer a new target for potential therapeutic intervention.

Introduction

Alzheimer's disease (AD) is characterized by the progressive decline of memory and cognition, with complicated pathological mechanisms. The two hallmarks of AD are the extracellular deposition of β-amyloid (Aβ) plaques and the intracellular accumulation of neurofibrillary tangles. In addition, the alteration of synaptic function, disruption of neuronal excitatory and inhibitory balance, and eventual neuronal loss are widely recognized pathogenic events occurring in AD (Palop and Mucke, 2010a, 2010b). It has been reported that the risk of unprovoked seizures is significantly higher in AD patients compared with nondemented controls (Hauser et al., 1986; Mendez et al., 1994; Hesdorffer et al., 1996; Lozsadi and Larner, 2006). Particularly, in AD patients with early onset dementia, the occurrence risk of epilepsy is 87-fold higher than control population during early stages (Amatniek et al., 2006), implicating neuronal hyperexcitability in disease pathogenesis. This is further supported by aberrant epileptiform activity and seizures in animal models of AD (Palop et al., 2007; Minkeviciene et al., 2009). Much research has been focused on glutamatergic excitatory synaptic system, whereas the inhibitory GABAergic synaptic system has received less attention.

In the vertebrate brain, GABA is the major inhibitory neurotransmitter that conveys its inhibitory effect through $GABA_A$ receptors (Moore, 1993; Lüscher and Keller, 2004). Emerging evidence indicates that the GABAergic synaptic system undergoes pathological changes. In a mouse model of AD, aberrant epileptic activity was also found associated with sprouting of inhibitory GABAergic synaptic terminals and enhanced synaptic inhibition,

Received April 18, 2017; revised July 22, 2017; accepted Aug. 14, 2017.

Author contributions: Y.L. and Hui Zheng designed research; Y.L., Z.C., Y.G., and G.P. performed research; Honghua Zheng, Y.-Z., H.X., G.B., and Hui Zheng contributed unpublished reagents/analytic tools; Y.L., Z.C., Y.G., G.P., and Hui Zheng analyzed data; Y.L. and Hui Zheng wrote the paper.

This work was supported by Natural Science Foundation of Fujian Province of China (Grant 2017J01151 and 2016J01411), the National Natural Science Foundation of China (Grant 81301105 and 81771164), National Institutes of Health (Grant R01 AG032051), and the National Key Research and Development Program of China (Grant 2016 YFC1305903).

The authors declare no competing financial interests.

Correspondence should be addressed to either Yanfang Li or Hui Zheng, Fujian Provincial Key Laboratory of Neurodegenerative Disease and Aging Research, Institute of Neuroscience, College of Medicine, Xiamen University, Xiamen, 361005 Fujian, China. E-mail: yfli@xmu.edu.cn or huiz@bcm.edu.

DOI:10.1523/JNEUROSCI.1051-17.2017

 0270-6474/17/379259-10$15.00/0

suggesting a compensatory response to the neuronal hyperexcitability. Dysregulated inhibition may interfere with synaptic function and contribute to learning and memory deficit in AD. Indeed, application of a $GABA_A$ receptor blocker has been shown to restore the cognitive deficient in animal models of AD (Marczynski, 1998; Yoshiike et al., 2008). However, the underlying mechanism for this inhibitory compensation is unclear.

Protocadherin-γC5 (Pcdh-γC5) is a member of clustered Pcdh-γ subfamily, which belongs to the well known cadherin family of synaptic adhesion molecules. Like cadherins, Pcdh members are hypothesized to engage homophilic or heterophilic interactions between adjacent cells. Pcdh-γs are predominantly expressed in the nervous system and have been reported to play important roles in neuronal connectivity, neurite self-avoidance, and neuron–astrocyte interactions, among others (Stoeckli, 2014; Keeler et al., 2015a, 2015b). We reported previously that Pcdh-γC5 interacts with $GABA_A$ receptors to promote its trafficking and GABAergic synaptic stabilization (Li et al., 2012). In the present study, we observed a significant increase of Pcdh-γC5 in amyloid precursor protein (APP)/presenilin-1 (PS1) mice and upon Aβ treatment *in vitro* and this was associated with elevated levels of GABAergic proteins and inhibitory synaptic function. Interestingly, Pcdh-γC5 can be induced under neuronal hyperexcitation conditions and knocking down endogenous Pcdh-γC5 rescued Aβ-induced synaptic dysfunction, supporting a critical role of Pcdh-γC5 in mediating synaptic function in AD pathogenesis.

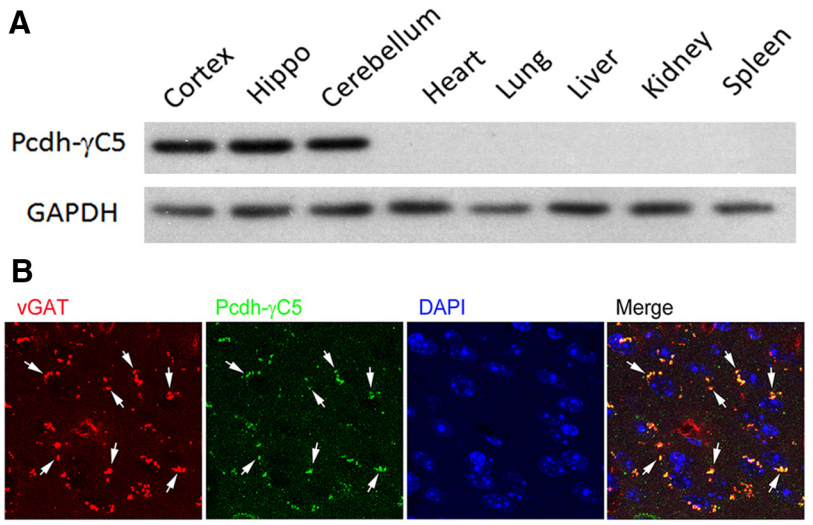

Figure 1. Expression analysis of Pcdh-γC5. ***A***, Western blot analysis using a house-made anti-Pcdh-γC5 antibody showing brain-specific expression of Pcdh-γC5. GAPDH blotting was used as a loading control. ***B***, Double immunostaining of brain slices with the anti-vGAT and anti-Pcdh-γC5 antibodies. DAPI was used as a counter strain. Arrows indicate representative vGAT and Pcdh-γC5 double-positive puncta.

Materials and Methods

Animals. The APPswe/PSEN1dE9 (APP/PS1) mice carrying mutations on both human APP and PS1 proteins were purchased from The Jackson Laboratory. The transgenic mice were backcrossed with C57BL/6 mice. Both female and male APP/PS1-transgenic mice and littermate wild-type (WT) mice were used in this study. For comparing the expression levels of Pcdh-γC5 and GABAergic markers between WT and APP/PS1 mice, both sexes of 9-month-old mice were used. For the immunofluorescence experiment, both sexes of 10- 13-month-old WT and APP/PS1 mice were used. Images were taken and quantified from two to three brain sections of each mouse. For electrophysiological recording with brain slices, both sexes of WT and APP/PS1 mice at ages as indicated were used. For the kainic acid (KA) injection experiment, male WT mice 2–4 months of age were used. The numbers of mice used for each experiment are specified in the figures and figure legends.

All experiments were performed in accordance with the National Institutes of Health's *Guidelines for the Care and Use of Laboratory Animals* and were approved by the Animal Ethics Committee of Xiamen University.

Antibodies and reagents. The rabbit anti-Pcdh-γC5 antibody was made in-house by immunization against aa 30–43 of mouse Pcdh-γC5 (GenBank accession no. NM_033583.3). The rabbit anti-APP antibody (Ru369) was developed as described previously. The mouse anti-vesicular GABA transporter (vGAT) antibody was from Santa Cruz Biotechnology (catalog #sc-393373). The rabbit anti-glutamate decarboxylase (GAD)65/67 antibody was from Millipore (catalog #AB1511). The mouse anti-β actin (catalog #ab8226) and rabbit anti-GAPDH (catalog #ab181602) antibodies were from Abcam. The mouse anti-vesicular glutamate transporter 1 (vGluT1) antibody was from Synaptic Systems (catalog #135511). All Alexa Flour-conjugated secondary antibodies for immunofluorescence were purchased from Invitrogen. The HRP-conjugated secondary antibodies for Western blotting were from Thermo Fisher Scientific. All reagents used for electrophysiological recording were from Sigma-Aldrich.

Western blotting. Briefly, the cortex was dissected from WT or APP/PS1 mice, followed by lysis with RIPA buffer (containing 10 mM Tris-HCl, 137 mM NaCl, 0.1% SDS, 1% Triton X-100, and 1% sodium deoxycholate, pH 7.4) and protease inhibitor. The homogenate was then centrifuged at 12,000 rpm for 20 min. The collected protein samples were separated with SDS-PAGE and transferred to PVDF membrane. The blots were then incubated with indicated primary antibodies at 4°C overnight and HRP-conjugated secondary antibodies at room temperature for 2 h, followed by detection with enhanced chemiluminescence (Millipore, catalog #WBKLSO500). The intensity of blotting bands was measured and quantified using ImageJ software.

RNA isolation and quantitative RT-PCR. Total RNA from mouse cortex or hippocampus was extracted using TRIzol reagent (Invitrogen, catalog #15596-018) and reverse transcribed to cDNA using GoScript Reverse transcription Kit (Promega, catalog #A5001). Quantitative RT-PCR was conducted using the Applied Biosystems (ABI) 7500.

The primers used for mouse gene expressions were as follows: vGAT forward: 5′-CATTCATTATCAGCGCGGCG-3′; vGAT reverse: 5′-AGCACGAACATGCCCTGA-3′; GAD65 forward: 5′-TCGGATCTGAAGATGGCTCTGC-3′; GAD65 reverse: 5′-TAGAGCAGAGCGCACAGCTT-3′; GAD67 forward: 5′-TTCCACTCCTTCGCCTGCA-3′; and GAD67 reverse: 5′-AGAAGCCACAGATCTTCAGGCC-3′.

Cell cultures and transfection. The HEK293T cells were maintained in high-glucose DMEM supplemented with 10% fetal bovine serum. For primary cortical neurons, the cortices of postnatal day 0 pups were isolated and diced to small pieces with forceps in ice-cold HBSS. Tissue was then transferred to fresh HBSS with 0.25% trypsin (Invitrogen, catalog #15090046) for digestion at 37°C for 15 min. Trypsin inhibitor (Invitrogen, catalog #17075029) was added to stop the reaction and tissue was collected after centrifugation at 3000 rpm for 2 min. Neuronal culture medium (Neurobasal A medium with 2% B27 supplement, 0.5 mM L-glutamine, 100 U/ml penicillin, and 0.1 mg/ml streptomycine) containing 0.1 mg/ml DNase (Sigma-Aldrich, catalog #D5025) was added to collected tissue and neurons were isolated by pipetting until there were no visible tissue clumps, centrifuging again, and resuspending the precipitate with fresh culture medium. Neurons were then seeded to poly-L-lysine-pretreated coverslips with the desired density and maintained in a 37°C incubator.

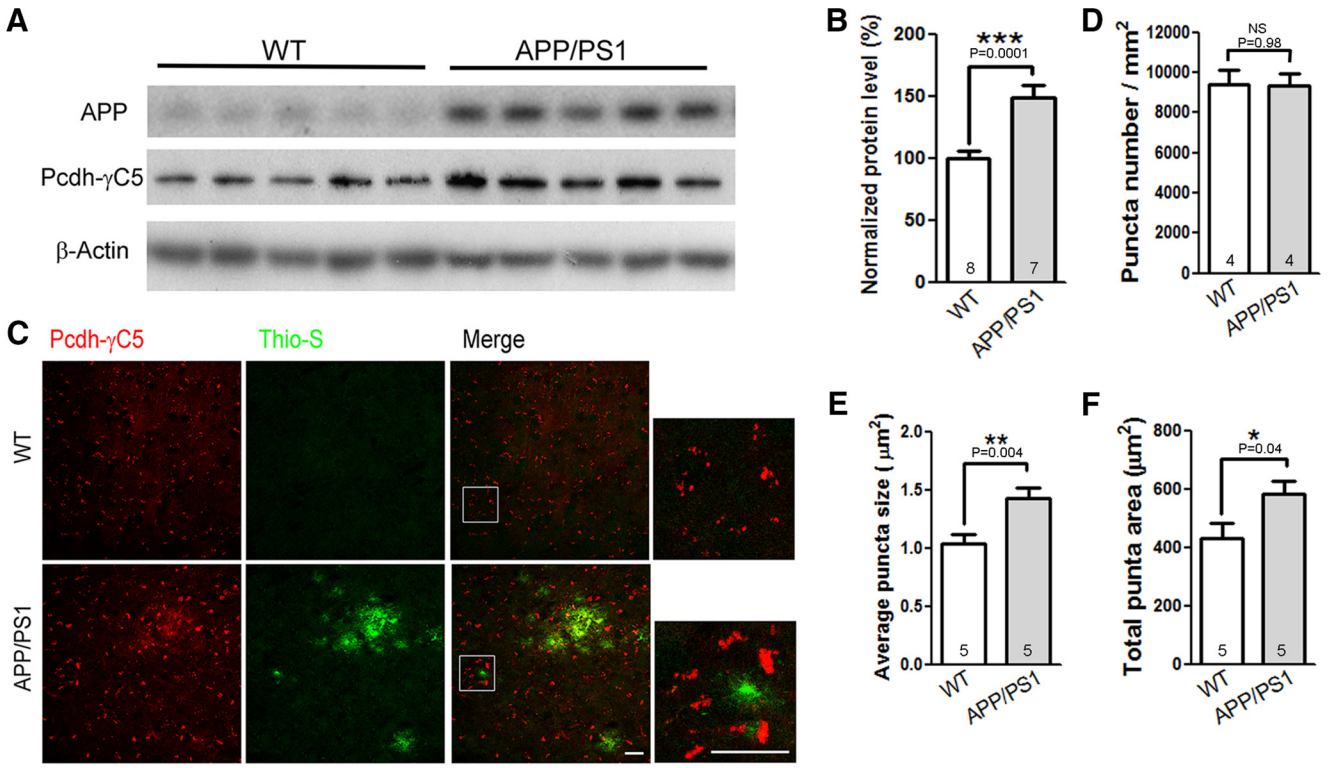

Figure 2. Increased expression of Pcdh-γC5 in APP/PS1 mice. ***A***, Western blot analysis of APP and Pcdh-γC5 expression in cortical homogenates of 9-month-old WT and APP/PS1 mice. β-actin was used as a loading control. ***B***, Quantification of relative Pcdh-γC5 levels (100.0 ± 6.8% WT vs 148.9 ± 10.1% APP/PS1). ***C***, Anti-Pcdh-γC5 and thioflavin-S (Thio-S) staining of cortical areas of 10- to 13-month-old WT and APP/PS1 mice, with enlarged merged images of Pcdh-γC5 punctas around Aβ plaques (Thio-S) shown on the right. (***D–F***) Quantification of Pcdh-γC5-positive puncta numbers (WT: 9372.4 ± 746.9 vs APP/PS1: 9354.2 ± 580.7 puncta/mm^2) (***D***), average puncta size (WT: 1.0 ± 0.1 vs APP/PS1: 1.4 ± 0.1 μm^2) (***E***), and total puncta area (WT: 429.8 ± 52.6 vs APP/PS1: 580.7 ± 46.6 μm^2) (***F***). $n = 4–5$ pairs of mice with a total of 12–15 brain sections were used for image quantification. *$p < 0.05$; **$p < 0.01$; ***$p < 0.001$. NS, Nonsignificant ($p > 0.05$). Scale bar, 20 μm.

Cells were transfected with various vectors using Lipofectamine 2000 transfection reagents (Invitrogen,catalog #11668027) and following the product protocol.

DNA constructs and RNA interference. The full-length mouse Pcdh-γC5 cDNA (GenBank accession no. NM_033583.3) was subcloned to pcDNA3.1/myc-His A vector with myc and His tags at the C terminus. The two small hairpin RNAs (shRNAs) of Pcdh-γC5 were synthesized and subcloned to LentiLox 3.7 (pLL3.7) vector containing an EGFP tag. The specific targeting region in Pcdh-γC5 is 5′-GGATAATGGTGACCCTTCA-3′.

Aβ oligomer preparation and treatment. Five hundred microliters of 1,1,1,3,3,3,-hexafluoro-2-propanol (HFIP) was added to 1 mg of lyophilized $A\beta_{1-42}$ peptide (Invitrogen, catalog #03-112), followed by 30 min of incubation at room temperature. The solutions were aliquoted into a 25 μl volume. HFIP was allowed to evaporate in open tubes in a fume hood and any remaining traces of HFIP were removed with gentle N_2 air blowing. The dried peptide was stored over desiccant at −80°C until use. Then, 10 μl of DMSO was added to each Aβ aliquot and pipetted thoroughly at room temperature. The freshly resuspended Aβ was diluted in 90 μl of ice-cold F12 cell culture medium to 100 μM concentration and transferred to 4°C for 24–36 h. The appropriate volume of prepared Aβ oligomer was added to the medium of cultured neurons to a final concentration of 1 μM and incubated for 2 h. The neurons were then subjected to electrophysiological recording or protein extraction.

Electrophysiological recording. For recordings on brain slices, WT or APP/PS1 mice were anesthetized and decapitated. The brains were quickly excised and cut into 400-μm-thick coronal slices with vibrating microtome (Leica VT1200S) in ice-cold ACSF containing the following (in mM): 126 NaCl, 18 $NaHCO_3$, 2.5 KCl, 1.2 NaH_2PO_4, 1.2 $CaCl_2$, 2.4 $MgCl_2$, and 11 glucose aerated with 95% O_2–5% CO_2. For mice older than 5 months, high-sucrose ACSF containing the following (in mM) 206 sucrose, 26 $NaHCO_3$, 2.5 KCl, 1.25 NaH_2PO_4, 2 $CaCl_2$, 2 $MgSO_4$, and 10 glucose was used instead. The slices were then transferred to continuously aerated ACSF and incubated at 32°C for 30 min and then at room temperature for at least 30 min. For recording, the slices were transferred to a recording chamber continuously perfused with aerated ACSF. For whole-cell recording of sEPSCs and sIPSCs, pipette solution contained the following (in mM): 140 $CsCH_3SO_3$, 2 $MgCl_2$, 5 TEA-Cl, 10 HEPES, 1 EGTA, 2.5 Mg-ATP, and 0.3 Na_2-GTP adjusted to pH 7.2–7.4 with CsOH. Spontaneous EPSCs (sEPSCs) were recorded at a holding potential of −70 mV and spontaneous IPSCs (sIPSCs) were recorded at a holding potential of 0 mV. For evoked spikes recording, the brain slices were perfused with ACSF and the glass pipette was filled with solution contained the following (in mM): 140 K-gluconate, 2 $MgCl_2$, 0.1 $CaCl_2$, 10 HEPES, 1.1 EGTA, 0.3 Na_2-GTP, and Na_2-ATP adjusted to pH 7.25 with KOH.

For sEPSCs and sIPSCs recording on cultured cortical neurons, coverslips seeded with neurons were transferred to the recording chamber perfused with ACSF and the same recording protocol described above was used. Recording data were collected with a Multi-Clamp 700B amplifier (Molecular Devices) using Clampex10 acquisition software (Molecular Devices), filtered at 1 kHz, sampled, and digitized with a Digidata 1440A (Molecular Devices). Raw data were analyzed offline with pClamp10.3 software. The frequency and amplitude of sEPSCs and sIPSCs were measured with Mini analysis software.

Immunofluorescence and amyloid plaque staining. Mice were anesthetized, followed by perfusion through ascending aorta with 0.9% saline and then 4% paraformaldehyde for fixation. Brains were excised and postfixed overnight in 4% paraformaldehyde at 4°C, then transferred to 30% sucrose for cryoprotection. Frozen brains were sectioned with a freezing microtome. Parasagittal brain sections of 15 μm thickness were incubated with PBS containing 2% normal goat serum and 0.3% Triton X-100 at room temperature for 1 h, followed by incubation with primary antibodies. After washing with PBS, the brain sections were incubated with a mixture of secondary antibodies in PBS for 1.5 h, followed by washes. If needed, sections were subjected to DAPI (Sigma-Aldrich,

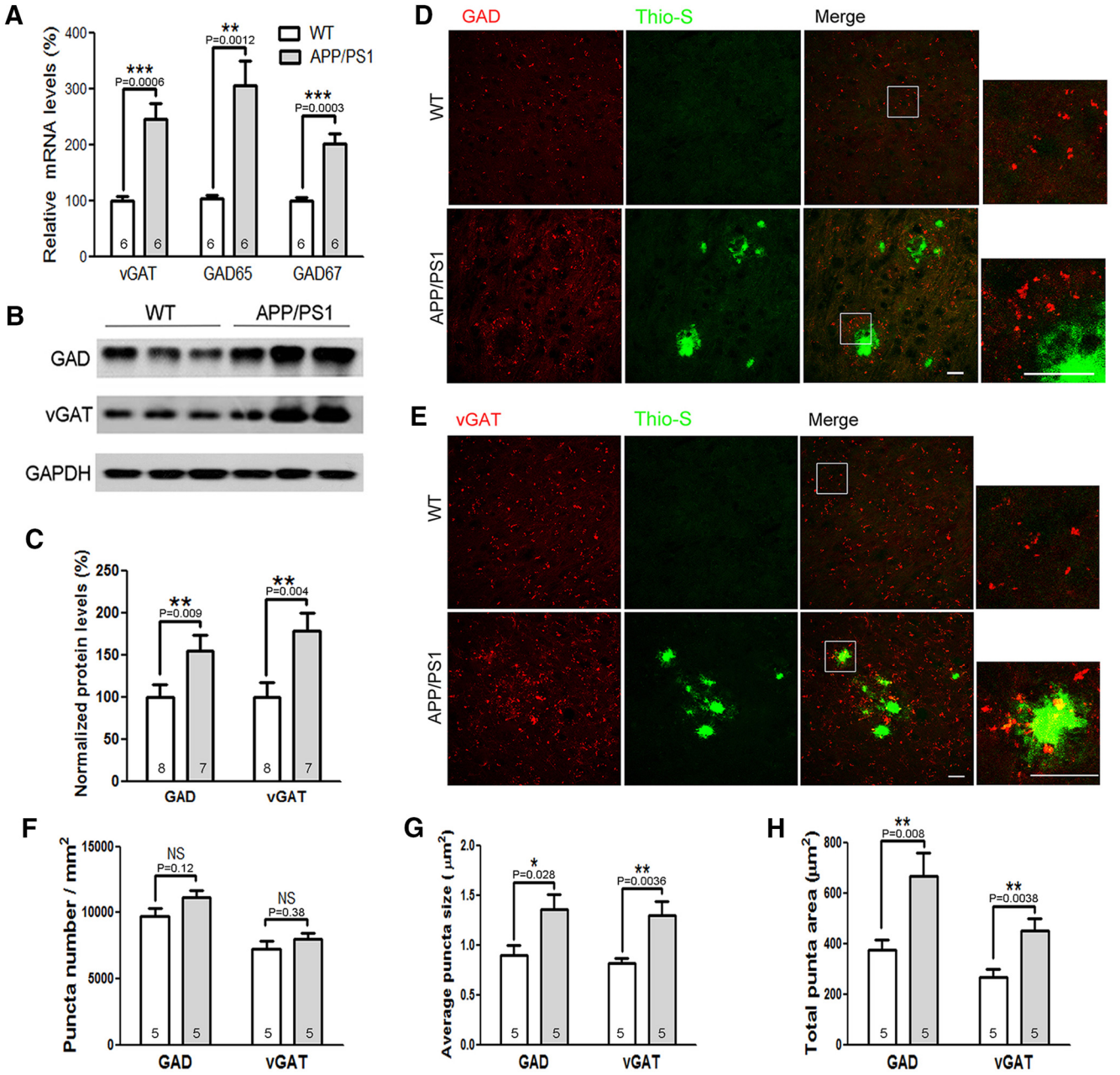

Figure 3. Increased levels of vGAT and GAD in APP/PS1 mice. ***A***, RT-PCR analysis of relative mRNA levels of the GABAergic synaptic markers vGAT, GAD65, GAD67 in cortical homogenates of WT and APP/PS1 mice at 9 months of age (vGAT: 246.4 ± 28.3%; GAD65: 305.9 ± 44.4%; GAD67: 201.9 ± 17.7% in APP/PS1 mice). ***B***, Western blot analysis of protein levels of GAD and vGAT of the same mice. ***C***, Quantification of ***B*** (GAD: 154.9 ± 18.5%; vGAT: 178.9 ± 20.3% in APP/PS1 mice). ***D***, ***E***, Immunostaining of GAD (***D***) and vGAT (***E***) with thioflavin-S (Thio-S) costaining in the cortex of 10 to 13-month-old WT and APP/PS1 mice. Images on right are enlarged merged images of GAD (***D***) or vGAT (***E***) punctas around Aβ plaques. ***F–H***, Quantification of GAD- and vGAT-positive puncta numbers (GAD: 9759.7 ± 604.4 vs 7977.2 ± 508.1 puncta/mm^2; vGAT: 7268.6 ± 604.4 vs 7977.2 ± 508.1 puncta/mm^2) (***F***), average puncta size (GAD: 0.89 ± 0.10 vs 1.35 ± 0.16 μm^2; vGAT: 0.82 ± 0.05 vs 1.30 ± 0.13 μm^2) (***G***), and total puncta area (GAD: 376.6 ± 38.8 vs 667.0 ± 90.5 μm^2; vGAT: 266.3 ± 31.4 vs 451.3 ± 45.7 μm^2) (***H***). $n = 5$ pairs of mice with a total of 12–15 brain sections were used for image quantification. *$p < 0.05$; **$p < 0.01$; ***$p < 0.001$. NS, Nonsignificant ($p > 0.05$). Scale bar, 20 μm.

catalog #D9542) staining for 10 min. To visualize amyloid plaques, brain sections were incubated with 1 mM thioflavine-S (Sigma-Aldrich, catalog #T1892) in 50% ethanol for 8 min, rinsed with 80% ethanol, and washed with PBS. After the staining, brain sections were mounted and analyzed by Nikon A1R laser confocal microscopy. Confocal microscopic images were analyzed using the ImageJ program. The original images were processed and converted into binary files and then the immunostained particles were analyzed, with puncta number, average puncta size, and total puncta area measured. The values were recorded and compared using Microsoft Excel and GraphPad Prism software.

Statistical analysis. Microsoft Excel or GraphPad Prism software was used for the statistical analyses. The data are presented as means ± SEM. When two groups were compared, raw data were analyzed by Student's *t* test. For comparison of various intensities of current-evoked spikes between WT and APP/PS1 mice, two-way ANOVA was used. $p < 0.05$ was considered statistically significant (*$p < 0.05$, **$p < 0.01$, ***$p < 0.001$). $p > 0.05$ was considered nonsignificant.

Results

Increased expression of Pcdh-γC5 and GABAergic synaptic markers in APP/PS1 mice

Pcdh-γC5 has been shown to play important roles in the brain, particularly in GABAergic inhibitory synaptic function and

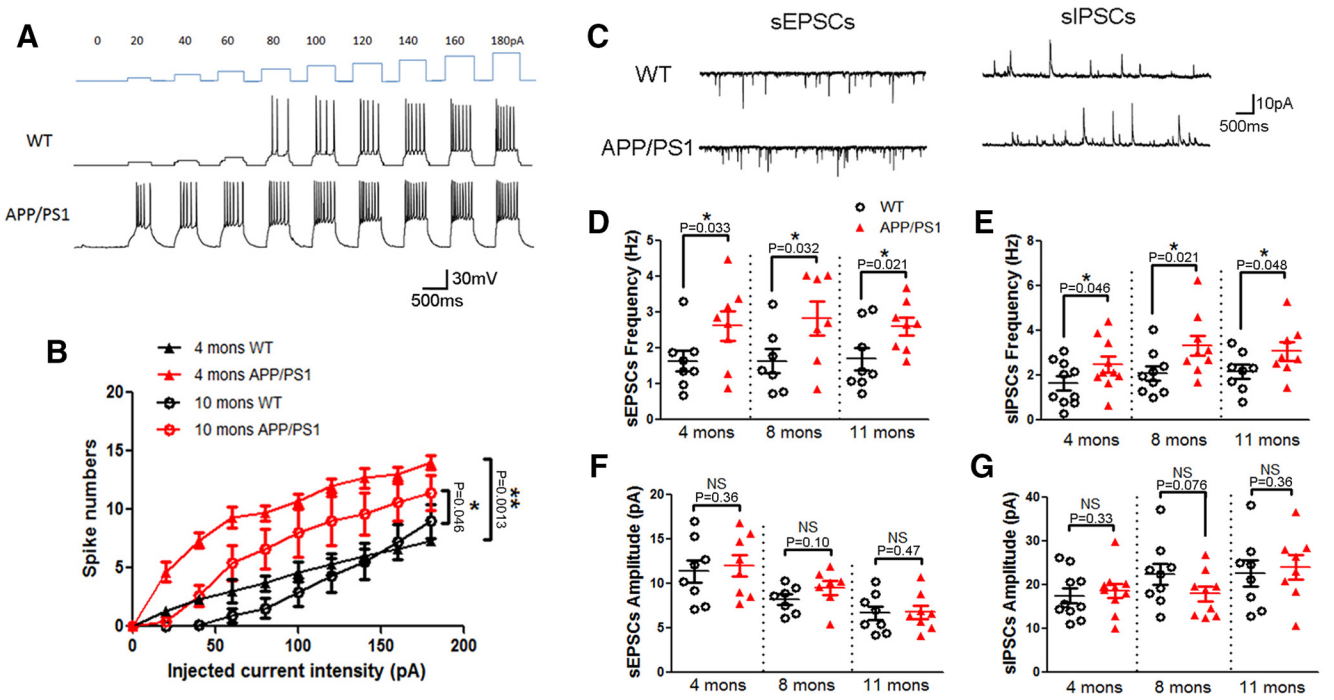

Figure 4. Aberrant neuronal excitation and inhibition in APP/PS1 mice. ***A***, Representative traces of evoked action potentials in response to various depolarization currents injected into individual cortical neurons of 10-month-old WT and APP/PS1 brain slices. ***B***, Quantification of evoked action potentials in 4- and 10-month-old WT and APP/PS1 mice. ***C***, Representative sEPSCs or sIPSCs in cortical neurons of 8-month-old WT and APP/PS1 mice. ***D***, Quantification of sEPSC frequency in cortical neurons of WT and APP/PS1 mice at various ages (1.63 ± 0.28 vs 2.61 ± 0.41 Hz at 4 months, 1.62 ± 0.34 vs 2.81 ± 0.47 Hz at 8 months, 1.68 ± 0.32 vs 2.59 ± 0.25 Hz at 11 months). ***E***, Quantification of sIPSC frequency (1.63 ± 0.31 vs 2.46 ± 0.36 Hz at 4 months, 2.07 ± 0.32 vs 3.31 ± 0.46 Hz at 8 months, 2.15 ± 0.30 vs 3.05 ± 0.41 Hz at 11 months). ***F***, Quantification of sEPSC amplitude (11.34 ± 1.27 vs 11.97 ± 1.24 pA at 4 months, 8.17 ± 0.59 vs 9.50 ± 0.79 pA at 8 months, 6.63 ± 0.76 vs 6.72 ± 0.75 pA at 11 months). ***G***, Quantification of sIPSC amplitude (17.42 ± 1.72 vs 18.50 ± 1.65 pA at 4 months, 22.26 ± 2.40 vs 17.83 ± 1.70 pA at 8 months, 22.54 ± 2.92 vs 23.98 ± 2.75 pA at 11 months). *$p < 0.05$; **$p < 0.01$. NS, Nonsignificant ($p > 0.05$).

maintenance. Consistent with this view, we found that Pcdh-γC5 was highly expressed in various regions of the brain including cortex, hippocampus and cerebellum, whereas its expression was negligible in non-neuronal tissues (Fig. 1*A*). Furthermore, double immunofluorescence staining using anti-Pcdh-γC5 and anti-vGAT antibodies revealed a high degree (~80%) of colocalization (Fig. 1*B*), indicating that Pcdh-γC5 is highly expressed in GABAergic neurons, where it is enriched in vesicular vGAT-positive presynaptic terminals.

Alteration of GABAergic transmission has been implicated in AD pathogenesis (Bareggi et al., 1982; Zimmer et al., 1984; Garcia-Marin et al., 2009; Gueli and Taibi, 2013; Ramos-Miguel et al., 2015), prompting us to examine Pcdh-γC5 expression in APP/PS1 mice, a commonly used animal model of AD. Interestingly, we detected significantly higher levels of Pcdh-γC5 in forebrain homogenates of 9-month-old APP/PS1 mice compared with WT littermate controls (Fig. 2*A*,*B*). Immunofluorescence staining of the cortex of 10- to 13-month-old APP/PS1 mice (Fig. 2*C*) revealed that, whereas the number of Pcdh-γC5-positive puncta was not affected (Fig. 2*D*), both the average puncta size (Fig. 2*E*) and total puncta area (Fig. 2*F*) were significantly increased in APP/PS1 mice. This was particularly the case in areas surrounding Aβ plaques (see enlarged views in Fig. 2*C*).

To determine whether elevated Pcdh-γC5 levels in APP/PS1 mice were associated with altered expression of GABAergic inhibitory synapse genes, we examined the expression of the GABAergic synaptic markers GAD and vGAT (Fig. 3). We found that both the mRNA (Fig. 3*A*) and protein levels (Fig. 3*B*, quantified in 3*C*) of GAD65 and GAD67, two isoforms of GAD, and vGAT were significantly higher in APP/PS1 mice compared with WT controls. This was supported by immunofluorescence staining of brain slices of the cortex of 10- to 13-month-old APP/PS1 mice (Fig. 3*D*,*E*). Although the puncta numbers of GAD and vGAT (Fig. 3*F*) did not change significantly, both the average puncta size (Fig. 3*G*) and total puncta area (Fig. 3*H*) were increased significantly compared with WT controls.

Enhanced neuronal excitation and inhibition in APP/PS1 mice

To further investigate the changes of synaptic function in APP/PS1 mice, electrophysiological recording was performed in brain slices from WT and APP/PS1 mice at different ages (Fig. 4). General neuronal excitation was determined using current-clamp recording by injecting positively charged current of various intensities into individual forebrain neurons to induce depolarization. At both 4 and 10 months of age, the current-induced spikes were significantly higher in APP/PS1 mice compared with WT controls (Fig. 4*A*,*B*). This was associated with higher sEPSCs and sIPSCs as measured by voltage-clamp recording (Fig. 4*C*–*G*). The frequency of both sEPSCs and sIPSCs were increased significantly in APP/PS1 mice at all ages tested (Fig. 4*D*,*E*), indicating increased neurotransmitter release from both excitatory and inhibitory presynaptic terminals. In contrast, the amplitude of sEPSCs and sIPSCs were comparable between genotypes (Fig. 4*F*,*G*), suggesting no significant change of postsynaptic glutamate or GABA receptors.

Neuronal hyperexcitation induces changes of Pcdh-γC5 and synaptic markers

Because sEPSCs are increased in APP/PS1 mice, the elevated Pcdh-γC5 and GABAergic markers and sIPSCs could either be independent of or secondary to neuronal excitation. To clarify

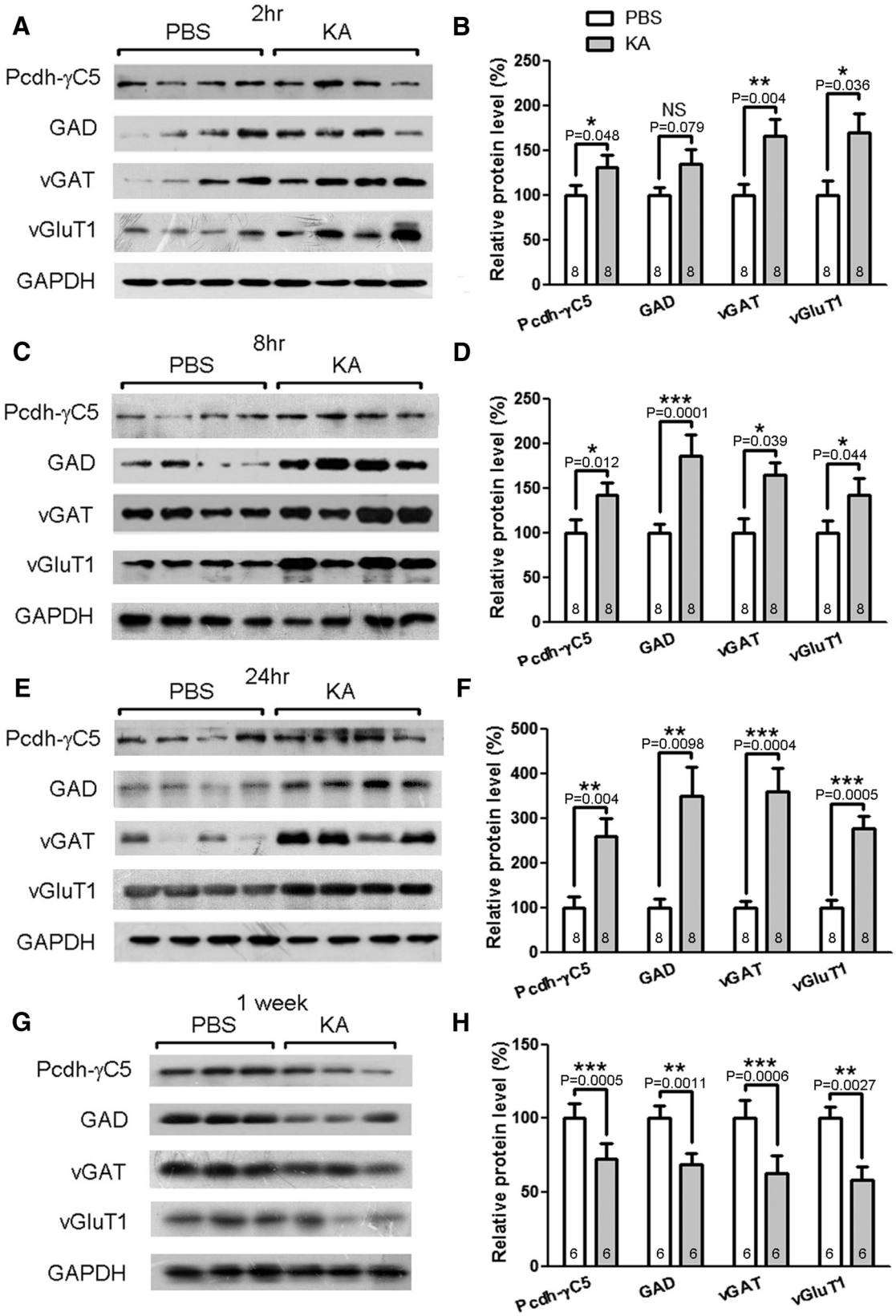

Figure 5. Western blot analysis of Pcdh-γC5 and the synaptic markers GAD, vGAT, and vGluT1 in the cortex of mice at different time points after KA injection. PBS, Vehicle control. ***A***, ***B***, Two hours after KA injection (Pcdh-γC5: 100.0 ± 11.3% vs 131.4 ± 12.9%; GAD: 100.0 ± 8.8% vs 134.5 ± 16.0%; vGAT: 100.0 ± 12.3% vs 165.8 ± 18.3%; vGluT1: 100.0 ± 15.6% vs 169.5 ± 21.8%). ***C***, ***D***, Eight hours after KA injection (Pcdh-γC5: 100.0 ± 14.1% vs 141.5 ± 14.0%; GAD: 100.0 ± 10.0% vs 186.0 ± 23.2%; vGAT: 100.0 ± 15.7% vs 164.7 ± 13.6%; vGluT1: 100.0 ± 12.7% vs 141.9 ± 18.7%). ***E***, ***F***, Twenty-four hours after KA injection (Pcdh-γC5: 100.0 ± 23.2% vs 258.1 ± 42.1%; GAD: 100.0 ± 18.9% vs 348.9 ± 64.4%; vGAT: 100.0 ± 14.6% vs 359.2 ± 51.2%; vGluT1: 100.0 ± 15.5% vs 276.3 ± 28.7%). ***G***, ***H***, One week after KA injection (Pcdh-γC5: 100.0 ± 10.0% vs 72.7 ± 10.2%; GAD: 100.0 ± 8.3% vs 68.9 ± 7.1%; vGAT: 100.0 ± 12.4% vs 63.1 ± 11.4%; vGluT1: 100.0 ± 7.6% vs 58.4 ± 9.1%). *$p < 0.05$; **$p < 0.01$; ***$p < 0.001$. NS, Nonsignificant ($p > 0.05$).

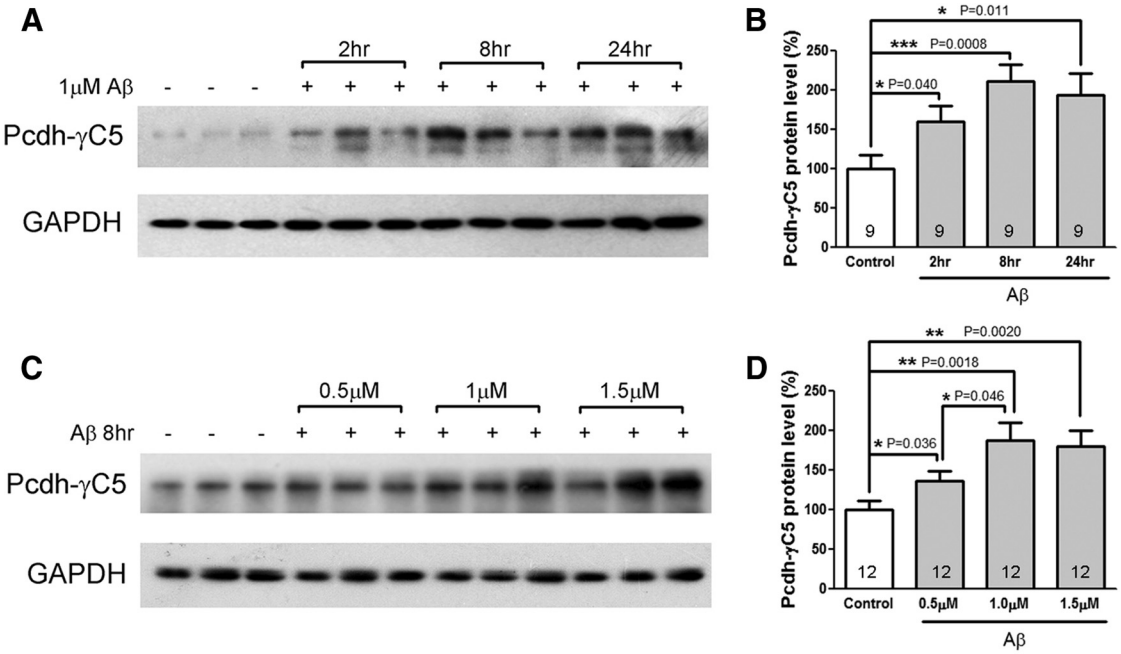

Figure 6. Aβ treatment increased the expression of Pcdh-γC5 in cortical neurons. ***A***, Western blot analysis of Pcdh-γC5 in cultured cortical neurons with 1 μM Aβ treatment for 2, 8, or 24 h or with DMSO for 24 h as a control. ***B***, Quantification of Pcdh-γC5 expression level in ***A*** (control: 100.0 ± 17.0%; 2 h: 159.2 ± 20.3%; 8 h: 210.8 ± 20.8%; 24 h: 193.6 ± 27.1%). ***C***, Western blot analysis of Pcdh-γC5 in cortical neurons treated with different concentrations of Aβ or DMSO as control for 8 h. ***D***, Quantification of Pcdh-γC5 expression level in ***C*** (control: 100.0 ± 11.4%; 0.5 μM Aβ: 136.1 ± 12.5%; 1.0 μM Aβ: 187.2 ± 22.3%; 1.5 μM Aβ: 179.9 ± 20.2%). *$p < 0.05$; **$p < 0.01$; ***$p < 0.001$.

the relationship between neuronal hyperexcitation and enhanced GABAergic synaptic function, we examined Pcdh-γC5 and GABAergic markers in a widely used KA-induced neuronal hyperexcitation model (Dibué et al., 2014), which induces acute epileptic behaviors after intraperitoneal injection of KA. The protein levels of Pcdh-γC5, the inhibitory presynaptic markers GAD and vGAT, and the excitatory presynaptic marker vGluT1 were determined at various time points after KA injection (Fig. 5). We observed increased levels of Pcdh-γC5 and inhibitory and excitatory proteins 2–24 h after KA treatment, followed by a reduction 1 week after KA treatment. Because neuronal excitation is the initial trigger, time-dependent increases of Pcdh-γC5 and inhibitory proteins support the idea that enhanced GABAergic synaptic function serves as a compensatory mechanism to counter hyperexcitation. However, sustained enhanced neurotransmitter release might lead to the depletion of synaptic vesicles, resulting in the eventual reduction of Pcdh-γC5 and synaptic markers observed 1 week after KA injection (Fig. 5*G*,*H*).

Aβ treatment increases the expression of Pcdh-γC5 in cortical neurons

It has been reported that Aβ could induce Ca^{2+} influx and elicit epileptiform activity in animal models of AD (Minkeviciene et al., 2009; Parodi et al., 2010). To investigate whether Aβ itself could trigger the alteration of Pcdh-γC5, cultured cortical neurons were treated with 1 μM oligomeric Aβ for different times. At all of the time points tested (2, 8, and 24 h), the expression levels of Pcdh-γC5 increased significantly compared with vehicle-treated controls (Fig. 6*A*,*B*), although there were no significant differences across time points. The effect of Aβ doses on Pcdh-γC5 was then tested by incubating the cortical neurons with different concentrations of oligomeric Aβ for 8 h. The expression of Pcdh-γC5 increased at all Aβ concentrations tested (0.5, 1.0, and 1.5 μM) and a significant dose-dependent effect was detected at doses between 0.5 and 1.0 μM (Fig. 6*C*,*D*). The results support the notion that the increased Pcdh-γC5 observed in APP/PS1 mice is due to Aβ overproduction.

Pcdh-γC5 modulates Aβ-induced synaptic dysfunction in cortical neurons

To provide mechanistic insights into Pcdh-γC5-mediated synaptic function, we designed a Pcdh-γC5 shRNA vector. The high efficiency knock-down was validated by transfecting a myc-tagged Pcdh-γC5 vector (Pcdh-γC5) or cotransfecting with Pcdh-γC5-myc and Pcdh-γC5 shRNA (Pcdh-γC5+sh) in HEK293 cells using pLL3.7 vector-cotransfected cells as a control (Fig. 7*A*,*B*). The effect of Pcdh-γC5 on synaptic function was investigated by whole-cell recording of cultured cortical neurons (Fig. 7*C*–*Q*). Knocking down Pcdh-γC5 expression decreased the frequency of both sEPSCs and sIPSCs significantly, but not the amplitude, indicating that Pcdh-γC5 modulates presynaptic neurotransmitter release directly (Fig. 7*C*–*G*). To determine whether Pcdh-γC5 could regulate Aβ-induced synaptic alteration, neurons were first transfected with Pcdh-γC5 shRNA or pLL3.7 control vector. Three days later, neurons were treated with 1 μM oligomeric Aβ for 2 h, followed by whole-cell recording (Fig. 7*H*–*L*). Consistent with the brain slices, Aβ treatment resulted in a higher frequency of sEPSCs and sIPSCs, but not amplitude. These effects were blunted by transfection with Pcdh-γC5 shRNA, suggesting that Pcdh-γC5 could regulate and rescue Aβ-induced synaptic changes efficiently.

We next investigated the effect of Pcdh-γC5 on cortical neurons from APP/PS1 mice, which generate more Aβ compared with WT mice. Neurons from APP/PS1 mice showed a significantly increased frequency of sEPSCs and sIPSCs. Similar to Aβ-treated neurons, knocking down Pcdh-γC5 efficiently rescued the frequency to normal levels, as recorded in WT neurons (Fig. 7*M*–*Q*), providing additional support that Aβ-induced synaptic dysfunction can be rescued by reducing Pcdh-γC5 expression.

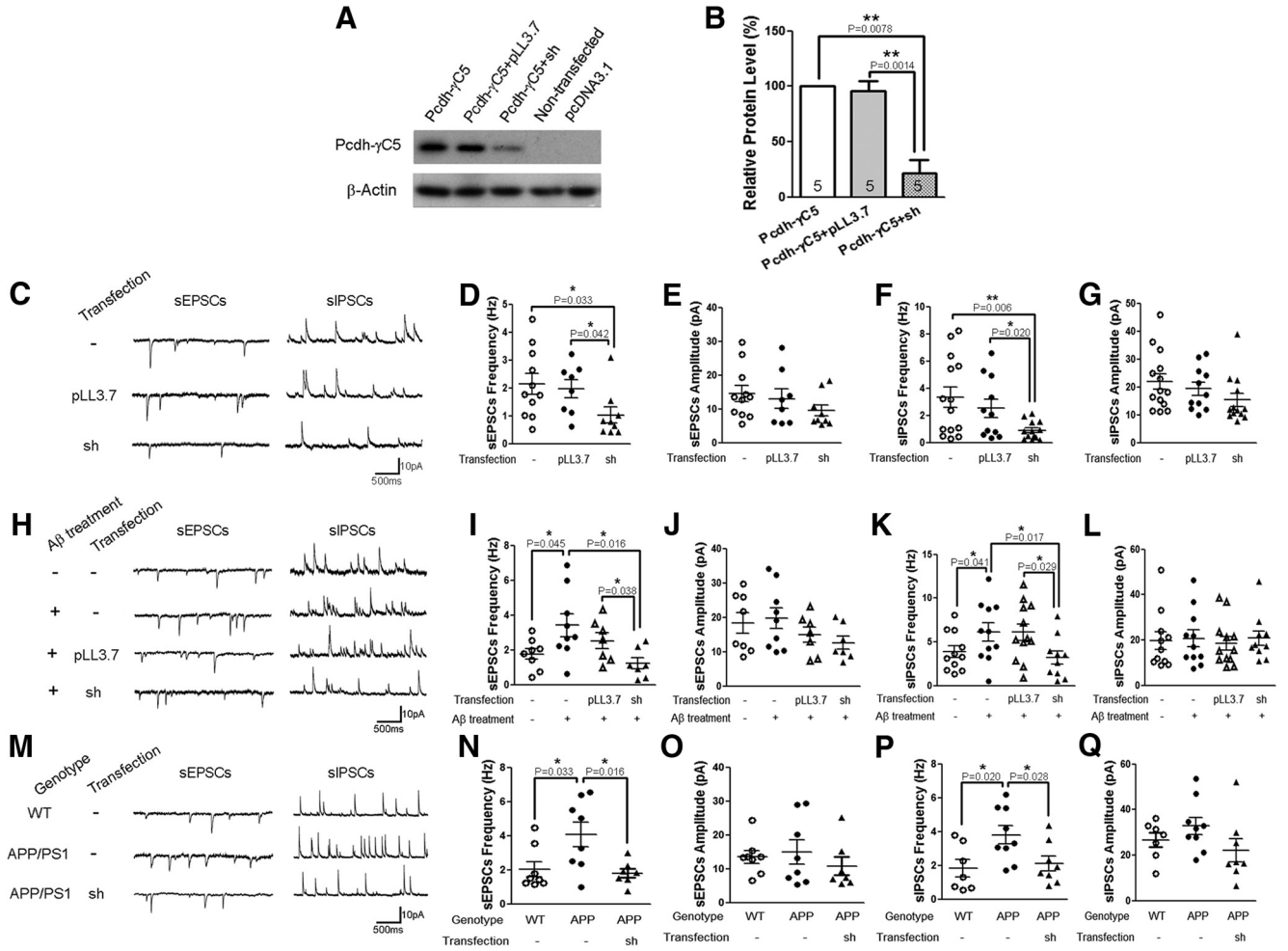

Figure 7. Knocking down Pcdh-γC5 rescued Aβ-associated sEPSCs and sIPSCs potentiation in cortical neurons. ***A***, ***B***, Pcdh-γC5 shRNA efficiently knocked down the expression of Pcdh-γC5 in transfected HEK293 cells (pLL3.7: 95.5 ± 9.1% of control; sh: 21.4 ± 12.3% of control). ***C***, Representative sEPSC and sIPSC traces of nontransfected cortical neurons (−) and neurons transfected with pLL3.7 vector or Pcdh-γC5 shRNA (sh). ***D***–***G***, Quantification of sEPSC frequency (nontransfected: 2.14 ± 0.37, pLL3.7: 1.96 ± 0.32, sh: 1.02 ± 0.29 Hz) (***D***), sEPSC amplitude (nontransfected: 14.53 ± 2.32, pLL3.7: 13.03 ± 2.89, sh: 9.51 ± 1.66 pA) (***E***), sIPSC frequency (nontransfected: 3.32 ± 0.76, pLL3.7: 2.52 ± 0.67, sh: 0.90 ± 0.19 Hz) (***F***), and sIPSC amplitude (nontransfected: 21.92 ± 2.81, pLL3.7: 19.39 ± 2.35, sh: 15.30 ± 2.38 pA) (***G***) showing reduced sEPSC and sIPSC frequency, but not amplitude, by Pcdh-γC5 shRNA. ***H***, Representative sEPSC and sIPSC traces of cortical neurons without transfection (−) or transfected with pLL3.7 vector (pLL3.7) or Pcdh-γC5 shRNA in the absence (−) of presence (+) of 1 μM oligomeric Aβ. ***I***–***L***, Quantification of sEPSC frequency (in conditions from left to right: 1.76 ± 0.31, 3.42 ± 0.66, 2.52 ± 0.47 and 1.21 ± 0.32 Hz) (***I***), sEPSC amplitude (18.36 ± 3.01, 19.73 ± 3.08, 19.94 ± 0.22 and 12.62 ± 1.95 pA) (***J***), sIPSC frequency (3.89 ± 0.67, 6.13 ± 1.02, 6.10 ± 0.95 and 3.17 ± 0.75 Hz) (***K***), and sIPSC amplitude (19.60 ± 3.88, 20.65 ± 3.71, 18.61 ± 2.96 and 20.78 ± 3.24 pA) (***L***) showing elevated sEPSC and sIPSC frequency by Aβ treatment and normalization by Pcdh-γC5 shRNA. The amplitude was not altered in all conditions. ***M***, Representative sEPSC and sIPSC traces of cortical neurons from WT or APP/PS1 mice without transfection (−) or transfected with Pcdh-γC5 shRNA. ***N***–***Q***, Quantification of sEPSC frequency (in conditions from left to right: 2.04 ± 0.44, 4.07 ± 0.73 and 1.80 ± 0.86 Hz) (***N***), sEPSC amplitude (13.47 ± 1.86, 14.92 ± 3.53 and 10.76 ± 2.70 pA) (***O***), sIPSC frequency (1.83 ± 0.51, 3.80 ± 0.53 and 2.10 ± 0.44 Hz) (***P***), and sIPSC amplitude (26.66 ± 3.17, 32.75 ± 3.80 and 22.08 ± 4.99 pA) (***Q***) showing elevated sEPSC and sIPSC frequency in APP/PS1 neurons and normalization by Pcdh-γC5 shRNA. The amplitude was not altered in all conditions. $^{*}p < 0.05$; $^{**}p < 0.01$.

Discussion

Compared with the pathological hallmarks of Aβ plaques and neurofibrillary tangles, synaptic dysfunction is known to best correlate with cognitive decline in AD (Palop and Mucke, 2016). In the past, considerable research has been focused on excitatory glutamatergic and cholinergic synaptic systems (Pozueta et al., 2013), whereas inhibitory GABAergic synapse systems received less attention because they were considered largely preserved in AD (Rossor et al., 1982; Reinikainen et al., 1988). However, emerging evidence implicates significant alteration and remodeling of GABAergic neurotransmission system in AD (Bareggi et al., 1982; Zimmer et al., 1984; Palop et al., 2007; Gueli and Taibi, 2013; Mitew et al., 2013; Jo et al., 2014; Wu et al., 2014; Zhan et al., 2014), which may contribute to overall network dysfunction. In this study, we show that the synaptic adhesion molecule Pcdh-γC5 is concentrated at GABAergic synaptic sites, where it mediates GABAergic synaptic transmission. Further, Pcdh-γC5 expression is elevated in APP/PS1 mice and in response to Aβ treatment and Pcdh-γC5 inhibition rescued the aberrant spontaneous synaptic currents induced by oligomeric Aβ and in neurons derived from APP/PS1 mice. The enhanced GABAergic synaptic function mediated by Pcdh-γC5 could act as a compensatory mechanism to neutralize the hyperexcitation induced by Aβ. However, sustained Pcdh-γC5 activation may result in the dysregulation of neuronal circuity and excitatory/inhibitory imbalance. Nevertheless, it is also possible that Pcdh-γC5, through its synaptic adhesion properties, modulates both excitatory and inhibitory activities in parallel. Regardless, our finding implicates a contribution of the Pcdh-γC5-dependent synaptic system in AD pathogenesis.

We have shown previously that Pcdh-γC5 interacts with $GABA_A$ receptors (Li et al., 2012). Our current results revealed that it colocalizes with presynaptic vGAT-positive puncta. This is in agreement with its characteristic as a synaptic adhesion molecule and the results combined support a model whereby presynaptic and postsynaptic Pcdh-γC5 interaction mediates synaptic transmission. Parallel increases in vGAT and GAD, which are specific GABAergic synaptic markers and responsible for presynaptic synthesis and release of neurotransmitter GABA, respectively, suggest that modulation of inhibitory synaptic function requires coordinated expression of multiple GABAergic proteins. In addition to the GABAergic neurons, Pcdh-γs was recently reported to interact with neuroligin-1 (Molumby et al., 2017), an adhesion protein mainly expressed in excitatory synapses. Therefore, it is conceivable that Pcdh-γC5 could modulate excitatory synaptic function independently or in corroboration with GABAergic neurons. In addition, Pcdhs have been documented to mediate the neuron–astrocyte interaction (Garrett and Weiner, 2009) and aberrant release of GABA from astrocytes has been reported to enhance neuronal tonic inhibition, leading to LTP deficit and cognitive impairment in AD-relevant settings (Mitew et al., 2013; Jo et al., 2014; Wu et al., 2014). Therefore, whether astrocytic Pcdh-γC5 also participates in GABAergic modulation is an interesting question and warrants further investigation.

We observed neuronal hyperexcitation and enhanced presynaptic neurotransmitter release in APP/PS1 mice. Enhanced GABAergic inhibition has been proposed as a compensatory mechanism to restore disrupted balance between inhibitory and enhanced excitatory activities in AD progression (Palop et al., 2007). Our data showing that direct induction of hyperexcitation by KA leads to upregulation of Pcdh-γC5 and the inhibitory markers vGAT and GAD is in support of this idea. It is also consistent with reports that Aβ treatment *in vitro* increases both neuronal excitability (Minkeviciene et al., 2009) and enhanced levels of functional $GABA_A$ receptors (Zhan et al., 2014). Pcdh-γs have been implicated in multiple neuronal functions, including cell survival, dendrite arborization, neurite self-avoidance, the neuron–astrocyte interaction, and the formation of functional neural circuits (Garrett et al., 2012; Stoeckli, 2014; Keeler et al., 2015a, 2015b). Like classic cadherins, Pcdh-γ family members undergo proteolytic processing by metalloproteinases and the γ-secretase, which results in the release of the intracellular domain, followed by its nuclear translocation and signal transduction (Haas et al., 2005; Hambsch et al., 2005; Junghans et al., 2005). Interestingly, the generation of cadherin intracellular domain in neurons could be stimulated by membrane depolarization or direct activation of NMDA receptors (Junghans et al., 2005; Reiss et al., 2005). Therefore, Pcdh-γC5 may sense neuronal hyperexcitation and initiate transcriptional regulation in a similar manner. However, diminished perisomatic GABAergic synaptic terminals were observed in the cortex of AD patients and APP/PS1 mice, especially around amyloid plaques (Garcia-Marin et al., 2009; Ramos-Miguel et al., 2015). In addition, through EEG recording, reduced gamma oscillatory activity due to interneuron impairment was also observed in hAPP mice (Verret et al., 2012). These apparent contradictory findings may be caused by differences in the mouse models or the timing of the experiment. Indeed, by studying various AD mouse models at different ages, it was reported that excitatory glutamatergic and inhibitory GABAergic synaptic terminals were increased at early ages but declined at late stages (Bell and Claudio Cuello, 2006; Marttinen et al., 2015).

In addition to Aβ-induced changes of GABAergic transmission, abnormal activation of GABAergic system was also found to participate in the hyperphosphorylation of tau and the formation of neurofibrillary tangles (Nykänen et al., 2012; Nilsen et al., 2013). In addition, using various human ApoE knock-in mouse models, it was revealed that ApoE4 specifically released from GABAergic interneurons, but not pyramidal neurons or astrocytes, is responsible for its deleterious effect on neuronal loss and cognitive deficit (Li et al., 2009; Knoferle et al., 2014; Tong et al., 2014). Together, these findings support a widespread role of GABAergic dysfunction in AD pathogenesis. It will be interesting to explore whether Pcdh-γC5 is also involved in these processes.

References

Amatniek JC, Hauser WA, DelCastillo-Castaneda C, Jacobs DM, Marder K, Bell K, Albert M, Brandt J, Stern Y (2006) Incidence and predictors of seizures in patients with Alzheimer's disease. Epilepsia 47:867–872. CrossRef Medline

Bareggi SR, Franceschi M, Bonini L, Zecca L, Smirne S (1982) Decreased CSF concentrations of homovanillic acid and gamma-aminobutyric acid in Alzheimer's disease: age- or disease-related modifications? Arch Neurol 39:709–712. CrossRef Medline

Bell KF, Claudio Cuello A (2006) Altered synaptic function in Alzheimer's disease. Eur J Pharmacol 545:11–21. CrossRef Medline

Dibué M, Kamp MA, Neumaier F, Steiger HJ, Hänggi D, Hescheler J, Schneider T (2014) Cardiac phenomena during kainic-acid induced epilepsy and lamotrigine antiepileptic therapy. Epilepsy Res 108:666–674. CrossRef Medline

Garcia-Marin V, Blazquez-Llorca L, Rodriguez JR, Boluda S, Muntane G, Ferrer I, Defelipe J (2009) Diminished perisomatic GABAergic terminals on cortical neurons adjacent to amyloid plaques. Front Neuroanat 3:28. CrossRef Medline

Garrett AM, Weiner JA (2009) Control of CNS synapse development by {gamma}-protocadherin-mediated astrocyte-neuron contact. J Neurosci 29:11723–11731. CrossRef Medline

Garrett AM, Schreiner D, Lobas MA, Weiner JA (2012) γ-protocadherins control cortical dendrite arborization by regulating the activity of a FAK/PKC/MARCKS signaling pathway. Neuron 74:269–276. CrossRef Medline

Gueli MC, Taibi G (2013) Alzheimer's disease: amino acid levels and brain metabolic status. Neurol Sci 34:1575–1579. CrossRef Medline

Haas IG, Frank M, Véron N, Kemler R (2005) Presenilin-dependent processing and nuclear function of g-protocadherins. J Biol Chem 280:9313–9319. CrossRef Medline

Hambsch B, Grinevich V, Seeburg PH, Schwarz MK (2005) {gamma}-Protocadherins, presenilin-mediated release of C-terminal fragment promotes locus expression. J Biol Chem 280:15888–15897. CrossRef Medline

Hauser WA, Morris ML, Heston LL, Anderson VE (1986) Seizures and myoclonus in patients with Alzheimer's disease. Neurology 36:1226–1230. CrossRef Medline

Hesdorffer DC, Hauser WA, Annegers JF, Kokmen E, Rocca WA (1996) Dementia and adult-onset unprovoked seizures. Neurology 46:727–730. CrossRef Medline

Jo S et al. (2014) GABA from reactive astrocytes impairs memory in mouse models of Alzheimer's disease. Nat Med 20:886–896. CrossRef Medline

Junghans D, Haas IG, Kemler R (2005) Mammalian cadherins and protocadherins: about cell death, synapses and processing. Curr Opin Cell Biol 17:446–452. CrossRef Medline

Keeler AB, Molumby MJ, Weiner JA (2015a) Protocadherins branch out: Multiple roles in dendrite development. Cell Adh Migr 9:214–226. CrossRef Medline

Keeler AB, Schreiner D, Weiner JA (2015b) Protein kinase C phosphorylation of a γ-protocadherin C-terminal lipid binding domain regulates focal adhesion kinase inhibition and dendrite arborization. J Biol Chem 290:20674–20686. CrossRef Medline

Knoferle J, Yoon SY, Walker D, Leung L, Gillespie AK, Tong LM, Bien-Ly N, Huang Y (2014) Apolipoprotein E4 produced in GABAergic interneurons causes learning and memory deficits in mice. J Neurosci 34:14069–14078. CrossRef Medline

Li G, Bien-Ly N, Andrews-Zwilling Y, Xu Q, Bernardo A, Ring K, Halabisky B, Deng C, Mahley RW, Huang Y (2009) GABAergic interneuron dysfunc-

tion impairs hippocampal neurogenesis in adult apolipoprotein E4 knockin mice. Cell Stem Cell 5:634–645. CrossRef Medline

Li Y, Xiao H, Chiou TT, Jin H, Bonhomme B, Miralles CP, Pinal N, Ali R, Chen WV, Maniatis T, De Blas AL (2012) Molecular and functional interaction between protocadherin-gammaC5 and GABAA receptors. J Neurosci 32:11780–11797. CrossRef Medline

Lozsadi DA, Larner AJ (2006) Prevalence and causes of seizures at the time of diagnosis of probable Alzheimer's disease. Dementia and geriatric cognitive disorders 22:121–124. CrossRef Medline

Lüscher B, Keller CA (2004) Regulation of GABAA receptor trafficking, channel activity, and functional plasticity of inhibitory synapses. Pharmacol Ther 102:195–221. CrossRef Medline

Marczynski TJ (1998) GABAergic deafferentation hypothesis of brain aging and Alzheimer's disease revisited. Brain Res Bull 45:341–379. CrossRef Medline

Marttinen M, Kurkinen KM, Soininen H, Haapasalo A, Hiltunen M (2015) Synaptic dysfunction and septin protein family members in neurodegenerative diseases. Mol Neurodegener 10:16. CrossRef Medline

Mendez MF, Catanzaro P, Doss RC, Arguello R, Frey WH 2nd (1994) Seizures in Alzheimer's disease: clinicopathologic study. J Geriatr Psychiatry Neurol 7:230–233. CrossRef Medline

Minkeviciene R, Rheims S, Dobszay MB, Zilberter M, Hartikainen J, Fülöp L, Penke B, Zilberter Y, Harkany T, Pitkänen A, Tanila H (2009) Amyloid beta-induced neuronal hyperexcitability triggers progressive epilepsy. J Neurosci 29:3453–3462. CrossRef Medline

Mitew S, Kirkcaldie MT, Dickson TC, Vickers JC (2013) Altered synapses and gliotransmission in Alzheimer's disease and AD model mice. Neurobiol Aging 34:2341–2351. CrossRef Medline

Molumby MJ, Anderson RM, Newbold DJ, Koblesky NK, Garrett AM, Schreiner D, Radley JJ, Weiner JA (2017) γ-Protocadherins interact with neuroligin-1 and negatively regulate dendritic spine morphogenesis. Cell Rep 18:2702–2714. CrossRef Medline

Moore RY (1993) Principles of synaptic transmission. Ann N Y Acad Sci 695:1–9. Medline

Nilsen LH, Rae C, Ittner LM, Götz J, Sonnewald U (2013) Glutamate metabolism is impaired in transgenic mice with tau hyperphosphorylation. J Cereb Blood Flow Metab 33:684–691. CrossRef Medline

Nykänen NP, Kysenius K, Sakha P, Tammela P, Huttunen HJ (2012) gamma-Aminobutyric acid type A (GABAA) receptor activation modulates tau phosphorylation. J Biol Chem 287:6743–6752. CrossRef Medline

Palop JJ, Mucke L (2010a) Amyloid-beta-induced neuronal dysfunction in Alzheimer's disease: from synapses toward neural networks. Nat Neurosci 13:812–818. CrossRef Medline

Palop JJ, Mucke L (2010b) Synaptic depression and aberrant excitatory network activity in Alzheimer's disease: two faces of the same coin? Neuromolecular Med 12:48–55. CrossRef Medline

Palop JJ, Mucke L (2016) Network abnormalities and interneuron dysfunction in Alzheimer disease. Nat Rev Neurosci 17:777–792. CrossRef Medline

Palop JJ, Chin J, Roberson ED, Wang J, Thwin MT, Bien-Ly N, Yoo J, Ho KO, Yu GQ, Kreitzer A, Finkbeiner S, Noebels JL, Mucke L (2007) Aberrant excitatory neuronal activity and compensatory remodeling of inhibitory hippocampal circuits in mouse models of Alzheimer's disease. Neuron 55:697–711. CrossRef Medline

Parodi J, Sepúlveda FJ, Roa J, Opazo C, Inestrosa NC, Aguayo LG (2010) Beta-amyloid causes depletion of synaptic vesicles leading to neurotransmission failure. J Biol Chem 285:2506–2514. CrossRef Medline

Pozueta J, Lefort R, Shelanski ML (2013) Synaptic changes in Alzheimer's disease and its models. Neuroscience 251:51–65. CrossRef Medline

Ramos-Miguel A, Hercher C, Beasley CL, Barr AM, Bayer TA, Falkai P, Leurgans SE, Schneider JA, Bennett DA, Honer WG (2015) Loss of Munc18-1 long splice variant in GABAergic terminals is associated with cognitive decline and increased risk of dementia in a community sample. Mol Neurodegener 10:65. CrossRef Medline

Reinikainen KJ, Paljärvi L, Huuskonen M, Soininen H, Laakso M, Riekkinen PJ (1988) A post-mortem study of noradrenergic, serotonergic and GABAergic neurons in Alzheimer's disease. J Neurol Sci 84:101–116. CrossRef Medline

Reiss K, Maretzky T, Ludwig A, Tousseyn T, de Strooper B, Hartmann D, Saftig P (2005) ADAM10 cleavage of N-cadherin and regulation of cell–cell adhesion and b-catenin nuclear signalling. EMBO J 24:742–752. CrossRef Medline

Rossor MN, Garrett NJ, Johnson AL, Mountjoy CQ, Roth M, Iversen LL (1982) A post-mortem study of the cholinergic and GABA systems in senile dementia. Brain 105:313–330. CrossRef Medline

Stoeckli ET (2014) Protocadherins: not just neuron glue, more too! Dev Cell 30:643–644. CrossRef Medline

Tong LM, Djukic B, Arnold C, Gillespie AK, Yoon SY, Wang MM, Zhang O, Knoferle J, Rubenstein JL, Alvarez-Buylla A, Huang Y (2014) Inhibitory interneuron progenitor transplantation restores normal learning and memory in ApoE4 knock-in mice without or with Abeta accumulation. J Neurosci 34:9506–9515. CrossRef Medline

Verret L, Mann EO, Hang GB, Barth AM, Cobos I, Ho K, Devidze N, Masliah E, Kreitzer AC, Mody I, Mucke L, Palop JJ (2012) Inhibitory interneuron deficit links altered network activity and cognitive dysfunction in Alzheimer model. Cell 149:708–721. CrossRef Medline

Wu Z, Guo Z, Gearing M, Chen G (2014) Tonic inhibition in dentate gyrus impairs long-term potentiation and memory in an Alzheimer's disease model. Nat Commun 5:4159. CrossRef Medline

Yoshiike Y, Kimura T, Yamashita S, Furudate H, Mizoroki T, Murayama M, Takashima A (2008) GABA(A) receptor-mediated acceleration of aging-associated memory decline in APP/PS1 mice and its pharmacological treatment by picrotoxin. PLoS One 3:e3029. CrossRef Medline

Zhan XQ, Yao JJ, Liu DD, Ma Q, Mei YA (2014) Abeta40 modulates GABA(A) receptor alpha6 subunit expression and rat cerebellar granule neuron maturation through the ERK/mTOR pathway. J Neurochem 128:350–362. CrossRef Medline

Zimmer R, Teelken AW, Trieling WB, Weber W, Weihmayr T, Lauter H (1984) Gamma-aminobutyric acid and homovanillic acid concentration in the CSF of patients with senile dementia of Alzheimer's type. Arch Neurol 41:602–604. CrossRef Medline